



Duplicated zebrafish (*Danio rerio*) inositol phosphatases *inpp5ka* and *inpp5kb* diverged in expression pattern and function

Dhyanam Shukla¹ · Brian M. Gural¹ · Edmund S. Cauley² · Namarata Battula¹ · Shorbon Mowla¹ · Brittany F. Karas¹ · Llion E. Roberts³ · Luca Cavallo¹ · Luka Turkalj¹ · Sally A. Moody⁴ · Laura E. Swan³ · M. Chiara Manzini¹

Received: 31 August 2022 / Accepted: 27 April 2023 / Published online: 15 May 2023
© The Author(s) 2023

Abstract

One hurdle in the development of zebrafish models of human disease is the presence of multiple zebrafish orthologs resulting from whole genome duplication in teleosts. Mutations in inositol polyphosphate 5-phosphatase K (*INPP5K*) lead to a syndrome characterized by variable presentation of intellectual disability, brain abnormalities, cataracts, muscle disease, and short stature. *INPP5K* is a phosphatase acting at position 5 of phosphoinositides to control their homeostasis and is involved in insulin signaling, cytoskeletal regulation, and protein trafficking. Previously, our group and others have replicated the human phenotypes in zebrafish knockdown models by targeting both *INPP5K* orthologs *inpp5ka* and *inpp5kb*. Here, we show that *inpp5ka* is the more closely related orthologue to human *INPP5K*. While both *inpp5ka* and *inpp5kb* mRNA expression levels follow a similar trend in the developing head, eyes, and tail, *inpp5ka* is much more abundantly expressed in these tissues than *inpp5kb*. In situ hybridization revealed a similar trend, also showing unique localization of *inpp5kb* in the pineal gland and retina indicating different transcriptional regulation. We also found that *inpp5kb* has lost its catalytic activity against its preferred substrate, PtdIns(4,5)P₂. Since most human mutations are missense changes disrupting phosphatase activity, we propose that loss of *inpp5ka* alone can be targeted to recapitulate the human presentation. In addition, we show that the function of *inpp5kb* has diverged from *inpp5ka* and may play a novel role in the zebrafish.

Keywords Inositol phosphatase · *INPP5K* · Zebrafish · Gene duplication

Introduction

Inositol polyphosphate 5-phosphatase K (*INPP5K* [MIM:607875]) is a highly conserved phosphatase that participates in the regulation of phosphoinositide (PI) signaling. Also referred to as skeletal muscle and kidney-enriched inositol phosphatase (*SKIP*), *INPP5K* is highly expressed in the brain, eyes, and muscles during development and adulthood (Ijuin et al. 2000; Gurung et al. 2003). In humans, homozygous or compound heterozygous mutations in *INPP5K* have been causally linked to a form of muscular dystrophy with cataracts and intellectual disability (MIM: 617404) also associated with short stature, and microcephaly with considerable variability in the age of onset and clinical presentation (Osborn et al. 2017; Wiessner et al. 2017; Yousaf et al. 2017; D'Amico et al. 2020; Hathazi et al. 2021). Similarities have been noted with Marinesco-Sjögren syndrome (MIM: 248800), a form of myopathy also associated with congenital cataracts, short stature, and cerebellar ataxia (Senderek et al. 2005; Krieger et al. 2013).

Communicated by Caroline Brennan.

Dhyanam Shukla, Brian M. Gural, and Edmund S. Cauley contributed equally to the study.

✉ M. Chiara Manzini
chiara.manzini@rutgers.edu

¹ Department of Neuroscience and Cell Biology and Child Health Institute of New Jersey, Rutgers Robert Wood Johnson Medical School, 89 French Street, CHINJ Rm 3274, New Brunswick, NJ 08901, USA

² Department of Biochemistry and Molecular Medicine, School of Medicine and Health Sciences, The George Washington University, Washington, DC, USA

³ Institute of Systems, Molecular and Integrative Biology, University of Liverpool, Liverpool, UK

⁴ Department of Anatomy and Cell Biology, School of Medicine and Health Sciences, The George Washington University, Washington, DC, USA

PIs are a category of lipid molecules that play crucial roles in signal transduction, ion channel regulation, cellular migration, membrane trafficking, vesicle transport, and many other processes (Di Paolo and De Camilli 2006; Balla 2013; Raghu et al. 2019). The seven unique members of this group are distinguished by their patterns of phosphorylation of the inositol head (PtdIns), which can occur at one or more of three positions (-3, -4, or -5). Production of PIs is regulated by an array of kinases and phosphatases (Balla 2013). INPP5K hydrolyzes the D-5 position of the inositol ring in both PtdIns(4,5)P₂ and PtdIns(3,4,5)P₃, with highest activity for PtdIns(4,5)P₂ (Ijuin et al. 2000; Vandeput et al. 2006; Davies et al. 2015). INPP5K is largely localized to the endoplasmic reticulum (ER) (Gurung et al. 2003; Dong et al. 2018) but can translocate to membrane ruffles as part of a complex with the glucose-regulated protein GRP78/BiP to negatively regulate insulin receptor signaling via phosphatidylinositol-3-kinase (PI3K) (Ijuin and Takenawa 2003; Ijuin et al. 2015, 2016a, b).

Multiple zebrafish (*Danio rerio*) models of *INPP5K* loss of function have been generated using morpholino oligonucleotides (MOs) targeting both paralogs, *inpp5ka* and *inpp5kb* (Osborn et al. 2017; Wiessner et al. 2017; Hathazi et al. 2021). However, when the genes were targeted independently, knockdown of *inpp5ka* was sufficient to yield phenotypes typical of neurological and muscular disorders, such as microphthalmia, microcephaly, shortened body, reduced touch-evoked motility, and myopathy. In contrast, *inpp5kb* MOs produced a mild phenotype in a small subset of morphants (Osborn et al. 2017). In addition, we found *inpp5ka* expression to be significantly higher than *inpp5kb* in zebrafish embryos at 2 days post fertilization (dpf) (Osborn et al. 2017). These findings suggested that *inpp5ka* may be the most conserved human paralog and *inpp5kb* function may have diverged.

Due to a genome duplication event in teleost fish, about 30% of zebrafish genes have a paralog (Howe et al. 2013), but duplicated genes often acquire differential expression and function (Postlethwait et al. 1998; Ravi and Venkatesh 2018). In this study, we sought to better characterize expression patterns and function of *inpp5ka* and *inpp5kb* to understand whether they diverged and support the development of better models of *INPP5K* mutations in humans. We show that both *inpp5ka* and *inpp5kb* have a dynamic developmental expression in the eyes, head, and tail, but found that *inpp5kb* is expressed at lower levels and specifically enriched in the pineal gland and the inner nuclear layer of the retina. In addition, *Inpp5kb* lost the majority of its phosphatase activity for PtdIns(4,5)P₂ which is the preferred substrate for INPP5K (Ijuin et al. 2000). Together, these data indicate that *inpp5ka* is the closest ortholog to *INPP5K* and suggest a unique role for *inpp5kb* within the zebrafish neural tissues.

Methods

Animal care

Maintenance and husbandry of zebrafish (*Danio rerio*) breeders and larvae were performed following protocols approved by the Institutional Animal Care and Use Committee of George Washington University and Rutgers University. All animals were from AB or EK backgrounds.

Protein alignments

Clustal Omega and Jalview were used to align the sequences for all transcripts and define conservation (Sievers et al. 2011). Percent identities between the human INPP5K (NP_057616.2), zebrafish *Inpp5ka* (NP_001082962.2), and *Inpp5kb* (XP_021335021.1) were calculated using Jalview (Waterhouse et al. 2009).

Quantitative PCR analysis

Samples were collected at 1, 2, 3, 4, 5, and 30 dpf and at 1-year-old for adults. Whole zebrafish embryos and larvae or micro-dissected tissue from eyes, head, and tails were pooled and RNA was extracted using the ReliaPrep RNA Miniprep System kit (Promega, Madison, WI). RNA was treated with DNase I (New England Biolabs) and complementary DNA (cDNA) was synthesized using the iScript cDNA Synthesis kit (Bio-Rad). 600 ng of cDNA per sample were analyzed via qPCR using the SsoFast EvaGreen Supermix (Bio-Rad) or Power UP SYBR Green Master Mix (Thermo Fisher). All reactions were run with 3 technical replicates and repeated on at least 3 biological replicates for 40 cycles on a QuantStudio 3 RealTime PCR system and recorded with QuantStudio Design and Analysis software. Custom primers were designed for *inpp5ka* (ex9_F: 5'-TGGGACTGGATTGGGTTAT-3'; ex10_R: 5'-GCTCCTCATTGAAAGACACC-3') and *inpp5kb* (ex2_F: 5'-CGACCACTGACCTCTATGTG-3'; ex3_R: 5'-ATGAGGAGGTGACTCCATGT-3') and house-keeping controls elongation factor 1 alpha *eef1a* (*eef1a*_F: 5'-GGGCAAGGGCTCCTTCAA-3'; *eef1a*_R: 5'-CGCTCGCCTTCAGTTTG-3') and riboprotein L18 *rpl18* (*rpl18*_F: 5'-GGCTAAGGTGATGTTTTCGTG-3'; *rpl18*_R: 5'-GCACATTGCCAATGTTTCAGC-3').

Whole-mount in situ hybridization

Full-length *inpp5ka* (NM_001089493.1) and *inpp5kb* (XM_021479346.1) cDNAs were cloned into the pCS2 + plasmid (Addgene). Digoxigenin-labeled sense and antisense probes were synthesized from the linearized

plasmids using the DIG RNA Labeling Kit (SP6/T7) (Roche/MilliporeSigma). Whole-mount ISH was performed as previously described (Yan et al. 2009). Expression patterns were confirmed in at least 5 independent embryos per probe and representative images are shown.

RNA scope analysis

Zebrafish larvae were euthanized at 5 dpf by tricaine methanesulfonate and fixed in fresh 4% PFA for 24 h at 4 °C. Larvae were rinsed with 1×PBS three times and cryoprotected with a 15% and 30% sucrose gradient with 0.025% sodium azide. The fish were embedded in tissue freeze medium (TFM) (General Data Healthcare) and frozen in 2-methyl butane with dry ice. Cryosections were performed using a Leica CM1850 UV Cryostat (Leica Microsystems) at 12 µm and mounted on SuperFrost Plus Slides (Fisher Scientific). The RNAscope assay was performed using the Multiplex Fluorescent Reagent Kit (Advanced Cell Diagnostics) according to the protocol provided for fixed-frozen tissue samples (UM 323,100). The following modifications were made: post fixation in 4% PFA at 4 °C was increased to 20 min, antigen retrieval was performed for 5 min using a microwave to help the target retrieval buffer reach boiling point, and RNAscope Protease Plus was used instead of RNAscope Protease III. The samples were hybridized using custom-designed RNAscope target probes for *inpp5ka* (Dr-inpp5ka-C1, Cat# 1,224,361-C1) and *inpp5kb* (Dr-inpp5kb-C2, Cat# 1,224,371-C2). In addition, two positive control genes were used for each target gene, *polr2a* (Dr-polr2a-C1) and *ppib* (Dr-ppib-C2). The negative control gene used in this experiment was DapB (DapB-C1,C2) expressed in *Bacillus subtilis*. We used the TSA Vivid Fluorophore 520 (Cat# 323,271) to develop the HRP-C1 signal and TS Vivid Fluorophore 650 (Cat# 323,273) to develop the HRP-C2 signal; both at a concentration of 1:750. Slides were coverslipped using ProLong™ Gold Antifade Mountant (Thermo Fisher). Images were taken using a Zeiss LSM800 confocal microscope and Zeiss Zen imaging software. Expression patterns were confirmed in at least 5 independent larvae per probe and representative images are shown.

Phosphatase assay

Full-length *inpp5ka* (NM_001089493.1) and *inpp5kb* (XM_021479346.1) cDNAs were generated by gene synthesis and cloned into the pGEX-1 to generate GST-fusion proteins (Genewiz/Azenta Life Sciences). GST-human INPP5K and GST were used as positive and negative controls respectively (Weissner et al. 2017). Constructs were transformed into BL21 DE3 pLysS, induced with 100µM IPTG overnight, and harvested by centrifugation. Cells were lysed in assay buffer (50 mM Tris-HCl [pH 7.5], 150 mM NaCl,

10 mM MgCl₂) plus 1% Triton X-100, EDTA-free protease inhibitors (Roche Diagnostics) and turbonuclease (Sigma). GST fusion proteins were affinity purified over glutathione sepharose 4B (GE Healthcare). After extensive washing, aliquots of beads were run on Coomassie gels to determine the abundance of full-length fusion proteins. Beads bearing equal amounts of fusion proteins were incubated in assay buffer containing 135 µM PtdIns(4,5)P₂diC8 or PtdIns(3,4,5)P₃diC8, including control wells with no enzyme or no substrate lipid, and incubated for 1 h at 37°C. Free phosphate was measured using the Malachite Green assay kit (Echelon Biosciences). Results of three independent experiments were presented as mean ± standard deviation. To minimize variability between purifications, all constructs were freshly prepared and purified in parallel for each experiment.

Results

Zebrafish and human INPP5K protein alignments

To determine whether *inpp5ka* and *inpp5kb* lead to functionally divergent proteins, we first analyzed their protein sequence. Protein sequence alignment of INPP5K (NP_057616.2), Inpp5ka (NP_001082962.2), and Inpp5kb (XP_021335021.1) revealed 45.8% and 43.9% identity between the human orthologue and Inpp5ka and Inpp5kb respectively, while the zebrafish proteins showed 62.2% identity with each other (Fig. 1). Higher conservation was present in the phosphatase domain with 49.7% amino acid sequence identity between the human protein and either zebrafish protein. It is important to note that while the primary isoforms listed above are the most similar to the human gene, both *inpp5ka* and *inpp5kb* have additional predicted transcripts that are not found in humans. One transcript has an alternative exon 1 (*inpp5ka*: XM_009291785.3 and *inpp5kb*: XM_021479345.1) adding an N-terminal sequence of 63 amino acids for Inpp5ka and 48 amino acids for Inpp5kb. A small 27 base pair alternative exon 9 was also identified in predicted transcripts both *inpp5ka* (XM_00557623.4) and *inpp5kb* (XM_005155275.4). All expression and functional analyses performed in this study were based on the sequence of the primary isoforms most similar to the human gene, but the design for the primer and probes did not exclude other predicted isoforms.

Divergent expression and localization of INPP5K orthologs in zebrafish larva

Analysis of *inpp5ka* and *inpp5kb* mRNA obtained from whole zebrafish embryos had shown higher expression of *inpp5ka* (Osborn et al. 2017). We used qPCR to quantify expression patterns throughout the first five days of

Hs INPP5K	1	-----MSSRKL--SGPKGRRLSIHVVTWNVASAAPPLDLSLLQLNRRNLNDIYVIGLQELNSGIISLLSDAAFND	70
Dr Inpp5ka	1	MEEDLSRALNSVSLETKDCKMENFGLYVVTWNVATAEPDDVNALLQLNSP-KKPDLYVIGLQEVRAAPLKFVSDLAIED	79
Dr Inpp5kb	1	-----MSAKVGSTGGHQAFLHMTWNVGTAEPPADVRSLQLDSQ-PTTDLYVIGLQEVNATPVRYISDLIAED	70
Hs INPP5K	71	SWSSFLMDVLSPLSFIKVSIVRMQGILLLVFAKYQHLPYIQILSTKSTPTGLFGYWGNGGVNICKLYGYVYSIINCHL	150
Dr Inpp5ka	80	SWSHLFMDTSLPLHYIKVSSIRMQGLLLFFSKLEHVFPFIRDIQVITYTRTGLYGYWGNGGVNICKLYGYVYSIINCHL	159
Dr Inpp5kb	71	TWSHLLMETLAPGEYIKVTSVRMQGLLLILFAKQVHLFPFIRDISTYTRTGLFGYWGNGGVSIVRFSYFGEMLCFLNCHL	150
Hs INPP5K	151	PPHISNNYQRLHFDRILEMNCCEGRDIPNILDHDLIIWFGDMNFRIEDFGLHFVRESIKNRCYGGWLWEKDQLSIKKHD	230
Dr Inpp5ka	160	TAHMNYASQVRVDEFEHILDAQNFKNTKTPHVLVDHKKVVFWDGDLNFRIEDHGMFLVRNCITSQRFNLLWPKDQLTMMKQKE	239
Dr Inpp5kb	151	AAHMYALQRMDEFYILDTEFDMFNTQVLDHKKVVFWDGDLNFRIADHGMFLRSSINNSRFNLLWDRDQLSMLKKKE	230
Hs INPP5K	231	PLLEFQEGRLFPPTYKFDNRNSNDYDTSEKKRKPATWDRILWRLKRPQAGPDPIPI-----PASH--FSLSLRG	299
Dr Inpp5ka	240	VILQFEEGRLDFQPTYKFDNRNSNDYDTSGKKRKPACDRILWRVNPASLTENTNEEPEKQEEEREDEFPLKMTQEY	319
Dr Inpp5kb	231	PILQFEEGRLRFRKPTYKFDNRSETYNTSGKKRKPATWDRILWRIPKPAETIEDEK-----SSTASSADDFSVKVTQDM	306
Hs INPP5K	300	YSSHMTYGISDHKPVSGTFDLELKLPLVSAPLIVLMPEDLWTVENDDMMVSYSSTSDFPSSPWDWIGLYKVGLRDVNDYVS	379
Dr Inpp5ka	320	YTSKMEYGISDHKPVIGIFRLELRKMYETPLVQVFAEGEWSADFDVITYRLLQAFASSAWDWIGLYKVGFKSVDYITY	399
Dr Inpp5kb	307	YTCDSYSGVSDHKPVIGTFNLEMRKKVETPLVALTVEGIWSEDAIFTYTILENFESSTFDWIGLYKIGFKSASDYSTF	386
Hs INPP5K	380	AWVGDSKVSCLNQLQVYIDISNIPTEDEFLCYYSNLSRVSIGSRPFQIPPGSLREDPLGEAQPI-----	448
Dr Inpp5ka	400	AWVKDDQVSFNEELFQVFMNKDEIPVLGGECVLCYYSNQLCIVGISQPFKVQESRAAI--EGLVPEININGLNQALAS	476
Dr Inpp5kb	387	AWVKDDEVAANGEVVMQMNKNELPLLAGDYVLGYFTNMQTLIAFSPNFQILESKRAV--MEGLVQENINGLEK----	459

Fig. 1 Protein alignment of INPP5K, Inpp5ka, and Inpp5kb highlighting conserved amino acids required for phosphatase activity. The start and end of the catalytic domain in the human protein are marked with large red arrowheads. Amino acids required for phosphatase

activity have been denoted with asterisks (*). Small arrowheads indicate residues that are altered by missense variants in humans. Hs, *Homo sapiens*; Dr, *Danio rerio*

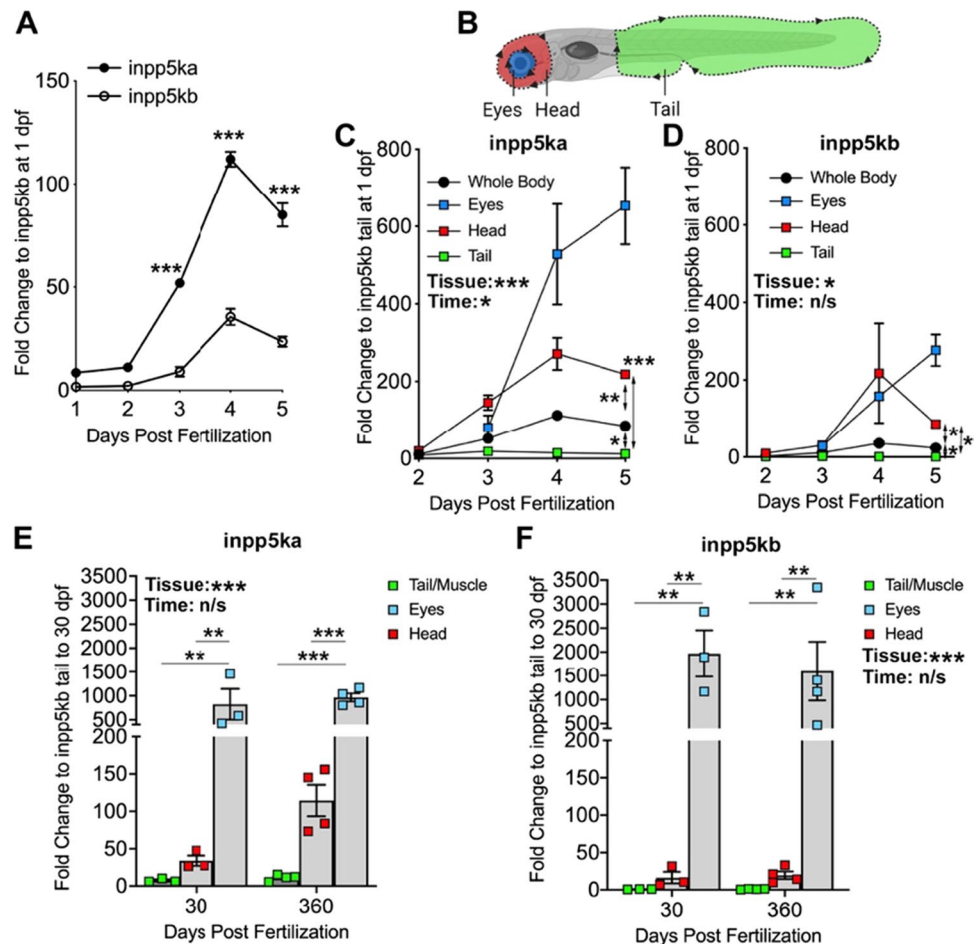
development. We found that *inpp5ka* (NM_001089493.1) was consistently expressed much more abundantly than *inpp5kb* (XM_021479346.1) (Fig. 2A). The developmental expression trend was similar for *inpp5ka* and *inpp5kb*. For comparison across the two genes fold changes for the whole embryo were quantified compared to *inpp5kb* expression at 1 dpf since it showed the lowest levels. Both genes showed relatively low levels at 1 and 2 dpf, but expression increased after 3 dpf and we saw 5.8, 3.2, and 3.6 higher expression of *inpp5ka* at 3, 4, and 5 dpf, respectively (Fig. 2A, fold change calculated to 1 dpf *inpp5kb*. *inpp5ka*: 1 dpf 8.5 ± 0.8 , 2 dpf 11.1 ± 1.5 , 3 dpf 51.9 ± 0.4 , 4 dpf 112.1 ± 3.6 , 5 dpf 84.9 ± 5.7 ; *inpp5kb*: 2 dpf 2.1 ± 0.1 , 3 dpf 9.0 ± 2.3 , 4 dpf 35.5 ± 3.9 , 5 dpf 23.6 ± 2.5 . $p > 0.0001$ at 3, 4, and 5 dpf).

Loss of *INPP5K* in humans affects the muscle, brain, and eyes and knockdown of *inpp5ka* in zebrafish larvae resulted in morphological abnormalities in the eyes and skeletal muscle (Osborn et al. 2017; Wiessner et al. 2017; Hathazi et al. 2021). We dissected the heads, eyes, and tails of developing larvae for tissue-specific expression analysis (Fig. 2B). Tissue-specific analysis revealed that, while *inpp5ka* was consistently expressed at higher levels than *inpp5kb*, both paralogs exhibit the greatest expression in the eyes, intermediate expression in the head, and low levels in the tail. For comparison, we calculated fold changes compared to expression levels of *inpp5kb* at 1 dpf. *inpp5ka* expression increased dramatically in the eyes by 5 dpf (Fig. 2C). Both genes showed similar increases in the head by 4 dpf with tail levels remaining consistently low (Fig. 2C, D, fold change relative to 1 dpf *inpp5kb* in the tail. *inpp5ka*: 3 dpf head

145.2 ± 19.3 , eyes 80.4 ± 31.6 ; 4 dpf head 271.2 ± 41.5 , eyes 528.1 ± 129.8 ; 5 dpf head 218.5 ± 2.7 , eyes 653.1 ± 99.6 . *inpp5kb*: 3 dpf head 30.4 ± 3.4 , eyes 28.6 ± 4.4 ; 4 dpf head 217.3 ± 128.8 , eyes 157.7 ± 8.4 ; 5 dpf head 85.8 ± 7.9 , eyes 276.9 ± 40.6). Since expression levels in the developmental time course seemed to be dropping after 4 dpf, we asked whether tissue-specific expression differences were still present in juvenile (30 dpf) and adult (1 year). Both *inpp5ka* and *inpp5kb* showed very high expression levels in the eyes which were comparable at both ages (Fig. 2E, F). mRNA expression in the head was higher for *inpp5ka* and increased in adulthood. While expression in the tail at 30 dpf and in dissected muscle at 1 year was low for *inpp5ka*, but still 7.6 to 11 times higher than *inpp5kb* (Fig. 2E, F, fold change relative to 30 dpf *inpp5kb* tail. *inpp5ka*: 30 dpf tail 7.6 ± 1.4 , head 33.9 ± 6.9 , eyes 828.9 ± 320.6 ; 360 dpf tail 11.3 ± 2.1 , head 114.5 ± 21.0 , eyes 965.9 ± 83.8 . *inpp5kb*: 30 dpf head 16.3 ± 7.1 , eyes 1967.1 ± 484.7 ; 360 dpf tail 0.99 ± 0.22 , head 19.6 ± 5.1 , eyes 1597.9 ± 615.8). Overall, *inpp5ka* showed consistently higher levels of expression than *inpp5kb* throughout the body apart from the eyes where expression of both genes was the highest at juvenile and adult timepoints.

To confirm the expression patterns, we first conducted in situ hybridization on whole-mount larvae at 3 dpf when expression begins to diverge. *inpp5ka* antisense probes reflected the results of qPCR expression assays. *inpp5ka* mRNA was most abundant in the head and eyes, with lower expression in the tail (Fig. 3A–C). As expected, *inpp5kb* antisense targeting revealed lower expression throughout the head and eyes (Fig. 3D, E). However, in contrast with

Fig. 2 *inpp5ka* and *inpp5kb* mRNAs differ in expression levels in zebrafish larvae. **A** Gene expression determined by qPCR. *inpp5ka* is more highly expressed in whole body lysates through 5 dpf. **B** Larval tissues were excised from the eye, head, and tail for localized gene expression analysis excluding the area of the trunk around the yolk. **C, D** Expression for both *inpp5ka* (**C**) and *inpp5kb* (**D**) is low in the tail and increases in the eyes and brain. By 5 dpf, both are most highly expressed in the eyes. Results from the whole body from (**A**) are shown as reference. **E, F *inpp5ka* (**E**) maintains higher expression levels than *inpp5kb* (**F**) in the tail/muscle and head at 30 dpf and in adult fish. Both genes are expressed at very high levels in the eyes. Values are averages \pm SEM. 2-way ANOVA results for tissue and developmental timepoint (time) are also listed. * $p < 0.05$, ** $p < 0.01$, *** $p < 0.001$**



inpp5ka, *inpp5kb* was abundantly expressed in the pineal gland (Fig. 3F), a neuroendocrine organ which responds to light and plays a role in circadian rhythm (Cahill 1996; Vantine et al. 2011; Livne et al. 2016). These findings suggested that in addition to lower expression, *inpp5kb* may have also diverged in its expression pattern. To better define the cellular distribution of the two mRNAs we then performed fluorescent RNA scope in situ on tissue cryosections at 5 dpf when expression levels are significantly increased via qPCR. This analysis revealed additional differences. *inpp5ka* was evenly distributed throughout the brain, in all layers of the retina, and was also present around the nuclei of lens cells (Fig. 4A, B). Expression in the muscle at the same exposure was much lower reflecting qPCR results (Fig. 4C). *inpp5kb* showed striking differences in distribution with very high expression in the pineal gland (Fig. 4D, Suppl. Fig. 1A) and in the inner nuclear layer of the retina (Fig. 4E, Suppl. Fig. 1B), though expression was still noted in the brain, other retinal layers, and the lens. As seen for *inpp5ka*, *inpp5kb* expression in the muscle was very low (Fig. 4F) though nuclei are sparse in this tissue and staining is less concentrated than in the brain and eyes (Suppl. Fig. 1C). Thus, the mRNA expression levels of *inpp5kb* in the brain and eye

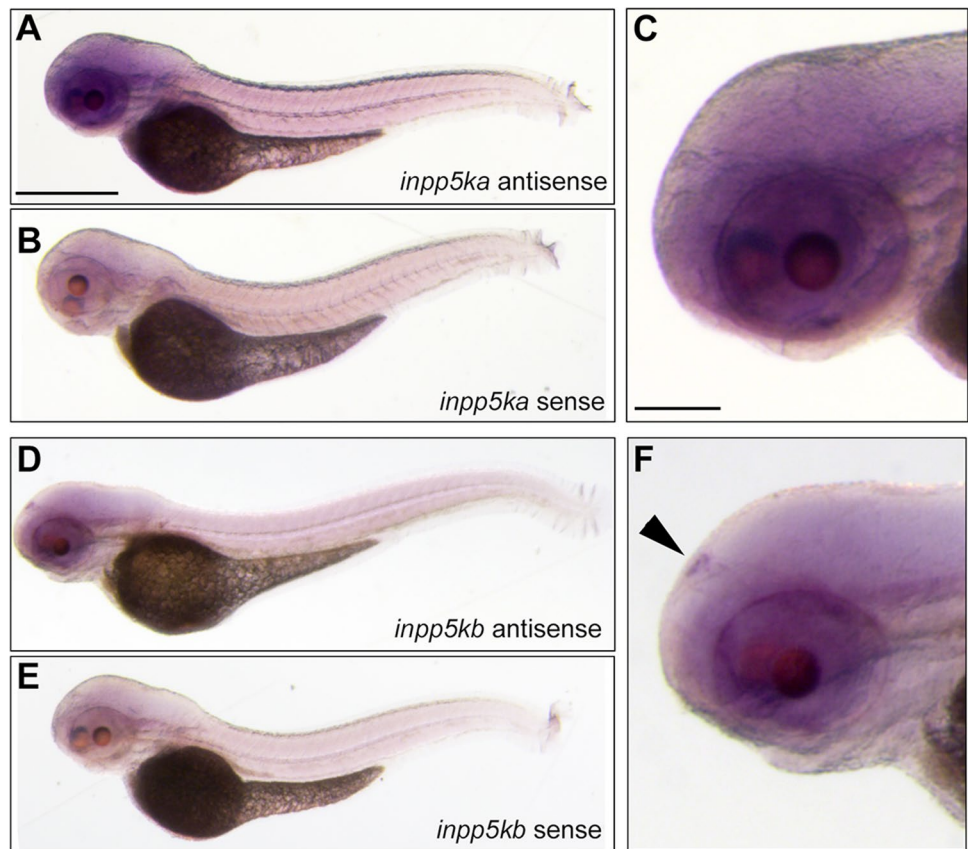
appear to be primarily driven by specific expression patterns while *inpp5ka* has a more even distribution pattern.

Divergence in phosphatase activity of human and zebrafish orthologs of INPP5K

To evaluate the preservation of the PI phosphatase activity in the zebrafish isoforms, we conducted a malachite phosphatase assay to examine the activity of INPP5K and the two zebrafish *Inpp5k* isoforms against PIP_3 and the preferred substrate $\text{PtdIns}(4,5)\text{P}_2$ (Fig. 5A). We found that zebrafish *Inpp5ka* and human INPP5K were both highly active against $\text{PtdIns}(4,5)\text{P}_2$ as expected. This activity was specific, as illustrated by the lack of phosphatase activity against PIP_3 . However, compared to *Inpp5ka*, *Inpp5kb* was nearly inactive against $\text{PtdIns}(4,5)\text{P}_2$. *Inpp5ka* yielded 409 pmol of free phosphate vs 20 pmol for *Inpp5kb*, indicating that *Inpp5ka* had a 20-fold higher activity compared to *Inpp5kb* (Fig. 5B).

The INPP5K protein is primarily composed of a 5-phosphatase domain between amino acids 16–318 and a SKITCH domain between amino acids 321–448. Most mutations identified in humans are missense and have been shown to reduce or ablate phosphatase activity (Osborn et al. 2017; Wiessner

Fig. 3 *inpp5ka* and *inpp5kb* mRNAs differ in localization at 3 dpf. **A–C** In situ hybridization in 3 dpf larvae shows that *inpp5ka* mRNA is highly expressed throughout the head and eyes. Scale bars: 500µm in (A), 100µm in (C). **D–F** *inpp5kb* expression is concentrated to the pineal gland. The pineal gland is indicated by the black arrow



et al. 2017). We wondered whether the loss in activity in Inpp5kb could be caused by changes in amino acids identified to be critical for the catalytic activity of INPP5K. Basing this analysis on the available crystal structures of other Type II inositol phosphate 5-phosphatases, *INPP5B* and *SYNJ1* (Tréaugues et al. 2014; Paesmans et al. 2020), we found that all sites were conserved in Inpp5ka and Inpp5kb and there were no major changes that could explain differences in activity (asterisks in Fig. 1). We also assessed whether residues known to be affected by pathogenic variants in patients were conserved in Inpp5kb, and these amino acids were all maintained (small arrowheads in Fig. 1) (D'Amico et al. 2020; Osborn et al. 2017; Hathazi et al. 2021; Wiessner et al. 2017; Yousaf et al. 2017). Thus, possible changes in known residues do not explain the difference in function between Inpp5ka and Inpp5kb.

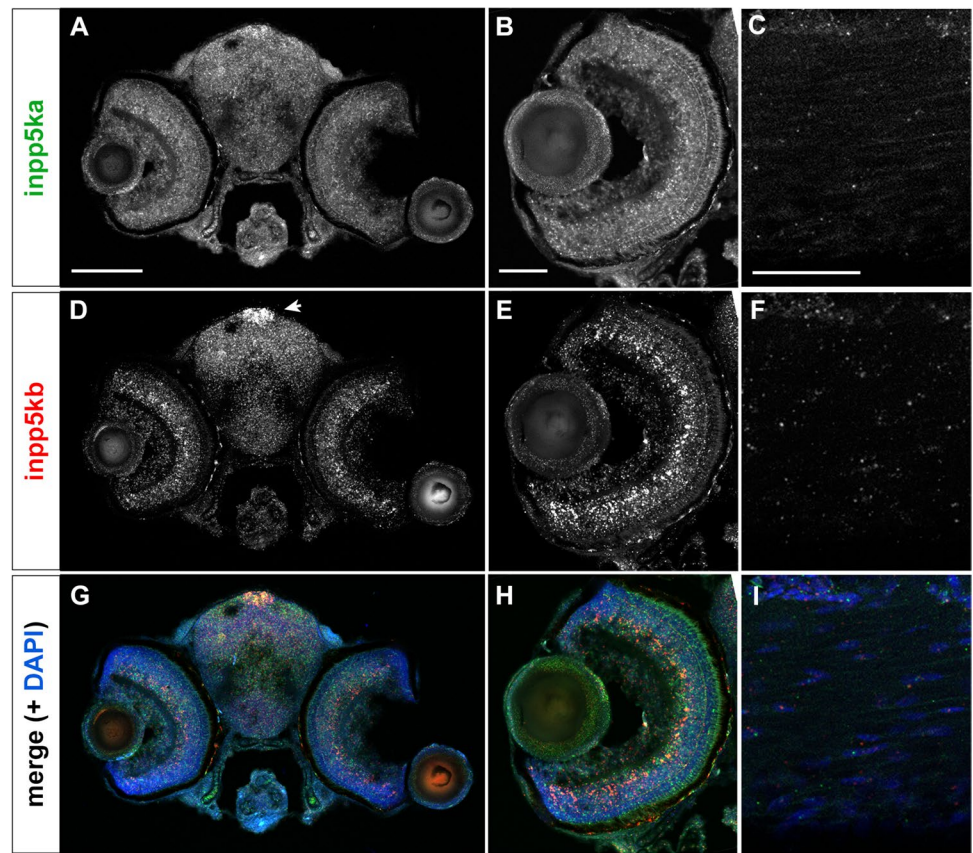
Discussion

INPP5K mutations in humans cause a distinct neurodevelopmental syndrome with variable presentation of intellectual disability, cataracts, short stature, and muscle disease (Osborn et al. 2017; Wiessner et al. 2017; Yousaf et al. 2017; D'Amico et al. 2020). Multiple zebrafish models have been

developed to study *inpp5ka/b* function using morpholino oligonucleotides either blocking translation or knocking down mRNA expression (Osborn et al. 2017; Wiessner et al. 2017; Hathazi et al. 2021). However, the presence of duplicated *inpp5k* genes, *inpp5ka* and *inpp5kb*, in zebrafish complicates the development of both candidate loss-of-function or point mutations zebrafish models since both orthologs may need to be targeted. Initial functional data from our previous studies had shown that *inpp5ka* knockdown alone was sufficient to replicate the findings in the double gene knockdown (Osborn et al. 2017). In this study, we show that *inpp5ka* and *inpp5kb* have diverged in expression levels, patterns, and function following teleost whole genome duplication (WGD). *inpp5ka*, rather than *inpp5kb*, maintains a higher sequence identity and similar expression pattern to human *INPP5K*, suggesting that genetic removal of this gene may be sufficient to recapitulate the human mutation.

Polyploidization by WGD is a significant driver of evolution (Postlethwait et al. 1998; Sémon and Wolfe 2007). During the period of re-diploidization that follows a WGD event, most redundant genes are eliminated via genomic rearrangements and mutations causing one duplicated copy to become a pseudogene. However, a duplicated gene may be preserved and gradually diverge in expression patterns and/or function during evolution leading to gene adaptation through

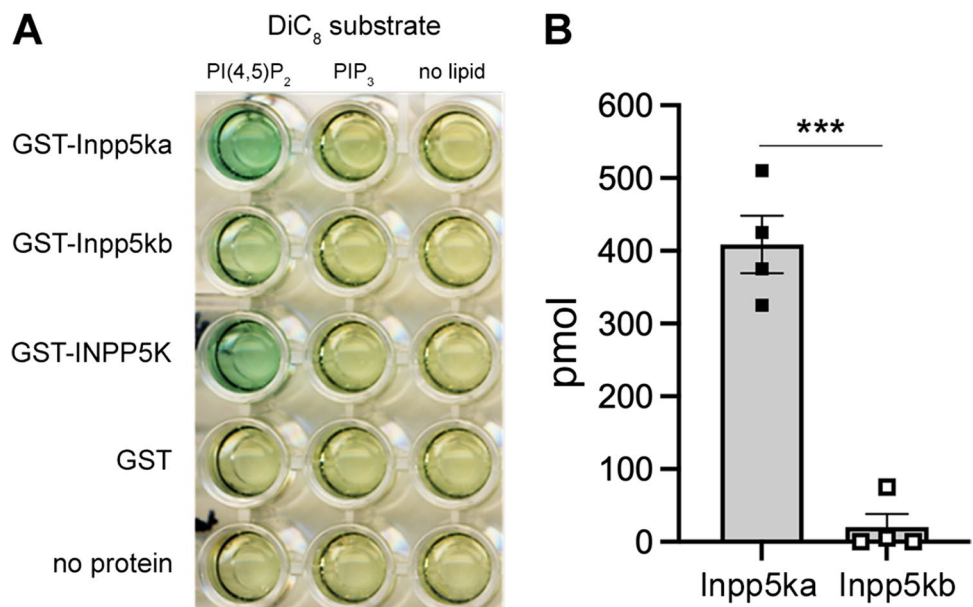
Fig. 4 Cellular distribution of *inpp5ka* and *inpp5kb* at 5 dpf by RNA scope in situ. **A–C** *inpp5ka* shows even distribution in the brain and eye (**A, B**), also labeling lens cells (**B**). Muscle expression is sparse and at lower levels (**C**). **D–F** *inpp5kb* brain expression is highest in the pineal gland (arrow in **D**). Increased expression is also noted in the inner nuclear layer of the retina with lower expression in photoreceptors, retinal ganglion cells, and lens cells (**E**, also see Suppl. Figure 1B). Sparse expression is present in muscle cells (**F**, also see Suppl. Fig. 1C). **G–I** Merged images including both probes (*inpp5ka* in green and *inpp5kb* in red) and DAPI to counterstain the nuclei. Scale bars: 100 μ m for (**A**), (**D**), and (**G**), 50 μ m for all other panels



sub-functionalization or neo-functionalization (Sémon and Wolfe 2007; Kassahn et al. 2009). While *inpp5ka* is broadly and highly expressed throughout the zebrafish larvae, *inpp5kb* is significantly less expressed. Interestingly, both genes show the highest expression in the eye which is maintained to adulthood. *inpp5ka* is evenly distributed

in retinal layers during development, matching the *Inpp5k* expression patterns identified in single-cell RNA sequencing (scRNAseq) datasets generated for the chick, and embryonic murine retina and the adult human retina (Lukowski et al. 2019; Balasubramanian et al. 2021; Yamagata et al. 2021). Considering that congenital cataracts are one of the

Fig. 5 *Inpp5ka* and *Inpp5kb* exhibit different phosphatase activity. **A** Phosphatase activity of human INPP5K, *Inpp5ka*, and *Inpp5kb* in the malachite assay. Human INPP5K and *Inpp5ka* demonstrate high activity for the $PI(4,5)P_2$ substrate. PIP_3 did not elicit activity from any isoform. **B** *Inpp5ka* is more significantly active against $diC8PI(4,5)P_2$ compared to *Inpp5kb*. Values are averages \pm SEM. *** $p < 0.001$ following a *t*-test



most consistent phenotypes linked to *INPP5K* mutations in humans (Osborn et al. 2017; Wiessner et al. 2017; Yousaf et al. 2017) the high expression of *inpp5ka* in lens cells found in the RNA scope experiments is also of note.

In contrast, we found that *inpp5kb* is highly enriched in the inner nuclear layer closer where amacrine cells and bipolar cells, both interneurons modulating the transmission of visual signals, are located (Connaughton et al. 2004; Zhao et al. 2009). Additional differential expression was found in the brain revealing widespread and sustained expression of *inpp5ka* while *inpp5kb* is highly enriched in the pineal gland. The pineal gland is thought to be the master regulator for circadian rhythm in vertebrates. Melatonin is the key circadian hormone secreted by the pineal gland in zebrafish (Cahill 1996) and is thought to play a role in locomotor activity (Livne et al. 2016), as well in the timing of reproduction and feeding (Piccinetti et al. 2013). It will be interesting in the future to determine the role of *Inpp5kb* in pineal and retinal functions independently of its phosphatase activity. This divergence in expression patterns further supports sub-functionalization of *inpp5kb*.

Additionally, we found that *Inpp5kb* exhibits minimal phosphatase activity against the traditional substrate of *INPP5K*, $\text{PtdIns}(4,5)\text{P}_2$ (Ijuin et al. 2000; Vandeput et al. 2006). In humans, much of the pathology resulting from mutations within *INPP5K* have been attributed to the dysregulation of phosphoinositide homeostasis (Osborn et al. 2017; Wiessner et al. 2017; McGrath et al. 2020; Hathazi et al. 2021). Most known mutations in *INPP5K* are missense variants occurring in the catalytic phosphatase domain reducing or ablating conversion of $\text{PtdIns}(4,5)\text{P}_2$ to $\text{PtdIns}(4)\text{P}$ (Osborn et al. 2017; Wiessner et al. 2017). In the muscle, *INPP5K* is involved in insulin signaling through the PI3K/Akt/mTOR pathway (Ijuin and Takenawa 2015; Ijuin et al. 2015), but studies in a muscle-specific *Inpp5k* mouse knock-out line also determined that abnormal accumulation of $\text{PtdIns}(4,5)\text{P}_2$ led to a severe disruption in lysosome recycling (McGrath et al. 2020). Interestingly, lysosome enlargement and autophagy inhibition found in the *Inpp5k*-deficient muscle were not dependent of Akt/mTOR signaling, suggesting an independent additional role for $\text{PtdIns}(4,5)\text{P}_2$ in muscle maintenance in the autophagic lysosome reformation pathway (McGrath et al. 2020). In addition, increased levels of D3-phosphoglycerate dehydrogenase (PHGDH) have been found in fibroblasts obtained from individuals with *INPP5K* phosphatase mutations, indicating further metabolic disruptions (Hathazi et al. 2021). It remains unclear whether *INPP5K* has additional functions independent of its phosphatase activity. It has been involved in endoplasmic reticulum (ER) organization by multiple groups

despite the absence of its substrates in the ER (Dong et al. 2018; Ramos et al. 2019). It is recruited there via interactions with the ER transmembrane protein ARL6IP1 but it is not known whether it is acting on neighboring membranes or performing other functions as part of a complex (Dong et al. 2018). Studies on the different functions and interactions of wild-type and phosphatase-dead zebrafish *Inpp5ka* and of *Inpp5kb* and their different isoforms may help shed light on the diverse subcellular activities of these proteins.

Overall, we propose that targeting the phosphatase domain in *Inpp5ka* would lead to a reliable model for *INPP5K* mutations in humans. Whether *Inpp5kb* evolved to perform a different function in specific subsets of cells and how it lost its phosphatase activity in the zebrafish remains to be studied.

Supplementary Information The online version contains supplementary material available at <https://doi.org/10.1007/s00427-023-00703-z>.

Acknowledgements The authors would like to thank all members of the Manzini laboratory for helpful discussion, Kathleen Flaherty and Heather Pond for management of the zebrafish colonies at Rutgers University and George Washington University, respectively, and Himani Majumdar for assistance with the in situ hybridization protocols.

Author contribution M.C.M. and E.S.C. conceived the study. D.S., B.M.G., E.S.C., L.E.R., S.M., N.B., B.F.K., L.C., and L.T. performed experiments and collected data. D.S., B.M.G., E.S.C., L.T., and M.C.M. analyzed the data. D.S., B.M.G., and M.C.M. wrote the manuscript with contributions from S.A.M. and L.E.S. All authors reviewed the manuscript.

Funding This work was funded by the National Institutes of Health R01NS109149 to M.C.M., Wellcome Trust (105616/Z/14/Z), and the Medical Research Council (MRC/N010035/1) to L.E.S. Additional support was provided to M.C.M. from the Robert Wood Johnson Foundation (grant #74260). B.F.K. was supported by training grant T32NS115700 from the National Institutes of Health.

Data availability All data generated or analyzed during this study are included in this published article.

Declarations

Competing interests The authors declare no competing interests.

Open Access This article is licensed under a Creative Commons Attribution 4.0 International License, which permits use, sharing, adaptation, distribution and reproduction in any medium or format, as long as you give appropriate credit to the original author(s) and the source, provide a link to the Creative Commons licence, and indicate if changes were made. The images or other third party material in this article are included in the article's Creative Commons licence, unless indicated otherwise in a credit line to the material. If material is not included in the article's Creative Commons licence and your intended use is not permitted by statutory regulation or exceeds the permitted use, you will need to obtain permission directly from the copyright holder. To view a copy of this licence, visit <http://creativecommons.org/licenses/by/4.0/>.

References

- Balasubramanian R, Min X, Quinn PMJ et al (2021) Phase transition specified by a binary code patterns the vertebrate eye cup. *Sci Adv* 7:eabj9846. <https://doi.org/10.1126/sciadv.abj9846>
- Balla T (2013) Phosphoinositides: tiny lipids with giant impact on cell regulation. *Physiol Rev* 93:1019–1137. <https://doi.org/10.1152/physrev.00028.2012>
- Cahill GM (1996) Circadian regulation of melatonin production in cultured zebrafish pineal and retina. *Brain Res* 708:177–181. [https://doi.org/10.1016/0006-8993\(95\)01365-2](https://doi.org/10.1016/0006-8993(95)01365-2)
- Connaughton VP, Graham D, Nelson R (2004) Identification and morphological classification of horizontal, bipolar, and amacrine cells within the zebrafish retina. *J Comp Neurol* 477:371–385. <https://doi.org/10.1002/cne.20261>
- D'Amico A, Fattori F, Nicita F et al (2020) A recurrent pathogenic variant of INPP5K underlies autosomal recessive congenital muscular dystrophy with cataracts and intellectual disability: evidence for a founder effect in Southern Italy. *Front Genet* 11:565868. <https://doi.org/10.3389/fgene.2020.565868>
- Davies EM, Kong AM, Tan A et al (2015) Differential SKIP expression in PTEN-deficient glioblastoma regulates cellular proliferation and migration. *Oncogene* 34:3711–3727. <https://doi.org/10.1038/onc.2014.303>
- Di Paolo G, De Camilli P (2006) Phosphoinositides in cell regulation and membrane dynamics. *Nature* 443:651–657. <https://doi.org/10.1038/nature05185>
- Dong R, Zhu T, Benedetti L et al (2018) The inositol 5-phosphatase INPP5K participates in the fine control of ER organization. *J Cell Biol* 217:3577–3592. <https://doi.org/10.1083/jcb.201802125>
- Gurung R, Tan A, Ooms LM et al (2003) Identification of a novel domain in two mammalian inositol-polyphosphate 5-phosphatases that mediates membrane ruffle localization. The inositol 5-phosphatase skip localizes to the endoplasmic reticulum and translocates to membrane ruffles following epidermal growth factor stimulation. *J Biol Chem* 278:11376–11385. <https://doi.org/10.1074/jbc.M209991200>
- Hathazi D, Cox D, D'Amico A, et al (2021) INPP5K and SIL1 associated pathologies with overlapping clinical phenotypes converge through dysregulation of PHGDH. *Brain* awab133. <https://doi.org/10.1093/brain/awab133>
- Howe K, Clark MD, Torroja CF et al (2013) The zebrafish reference genome sequence and its relationship to the human genome. *Nature* 496:498–503. <https://doi.org/10.1038/nature12111>
- Ijuin T, Takenawa T (2003) SKIP negatively regulates insulin-induced GLUT4 translocation and membrane ruffle formation. *Mol Cell Biol* 23:1209–1220. <https://doi.org/10.1128/mcb.23.4.1209-1220.2003>
- Ijuin T, Takenawa T (2015) Improvement of insulin signaling in myoblast cells by an addition of SKIP-binding peptide within Pak1 kinase domain. *Biochem Biophys Res Commun* 456:41–46. <https://doi.org/10.1016/j.bbrc.2014.11.031>
- Ijuin T, Mochizuki Y, Fukami K et al (2000) Identification and characterization of a novel inositol polyphosphate 5-phosphatase. *J Biol Chem* 275:10870–10875
- Ijuin T, Hatano N, Hosooka T, Takenawa T (2015) Regulation of insulin signaling in skeletal muscle by PIP3 phosphatase, SKIP, and endoplasmic reticulum molecular chaperone glucose-regulated protein 78. *Biochem Biophys Res Commun* 453:3192–3201. <https://doi.org/10.1016/j.bbrc.2015.09.009>
- Ijuin T, Hatano N, Takenawa T (2016a) Glucose-regulated protein 78 (GRP78) binds directly to PIP3 phosphatase SKIP and determines its localization. *Genes to Cells* 21:457–465. <https://doi.org/10.1111/gtc.12353>
- Ijuin T, Hosooka T, Takenawa T (2016b) Phosphatidylinositol 3,4,5-trisphosphate phosphatase SKIP links endoplasmic reticulum stress in skeletal muscle to insulin resistance. *Mol Cell Biol* 36:108–118. <https://doi.org/10.1128/mcb.00921-15>
- Kassahn KS, Dang VT, Wilkins SJ et al (2009) Evolution of gene function and regulatory control after whole-genome duplication: Comparative analyses in vertebrates. *Genome Res* 19:1404–1418. <https://doi.org/10.1101/gr.086827.108>
- Krieger M, Roos A, Stendel C et al (2013) SIL1 mutations and clinical spectrum in patients with Marinesco-Sjögren syndrome. *Brain* 136:3634–3644. <https://doi.org/10.1093/brain/awt283>
- Livne ZB-M, Alon S, Vallone D et al (2016) Genetically blocking the zebrafish pineal clock affects circadian behavior. *Plos Genet* 12:e1006445. <https://doi.org/10.1371/journal.pgen.1006445>
- Lukowski SW, Lo CY, Sharov AA et al (2019) A single-cell transcriptome atlas of the adult human retina. *Embo J* 38:100811. <https://doi.org/10.15252/embj.2018100811>
- McGrath MJ, Eramo MJ, Gurung R, et al (2020) Defective lysosome reformation during autophagy causes skeletal muscle disease. *J Clin Invest* 131. <https://doi.org/10.1172/jci135124>
- Osborn DPS, Pond HL, Mazaheri N et al (2017) Mutations in INPP5K cause a form of congenital muscular dystrophy overlapping Marinesco-Sjögren syndrome and dystroglycanopathy. *Am J Hum Genet* 100:537–545. <https://doi.org/10.1016/j.ajhg.2017.01.019>
- Paesmans J, Martin E, Deckers B et al (2020) A structure of substrate-bound Synaptojanin1 provides new insights in its mechanism and the effect of disease mutations. *Elife* 9:e64922. <https://doi.org/10.7554/elife.64922>
- Piccinetti CC, Migliarini B, Olivetto I et al (2013) Melatonin and peripheral circuitries: insights on appetite and metabolism in Danio rerio. *Zebrafish* 10:275–282. <https://doi.org/10.1089/zeb.2012.0844>
- Postlethwait JH, Yan YL, Gates MA et al (1998) Vertebrate genome evolution and the zebrafish gene map. *Nat Genet* 18:345–349. <https://doi.org/10.1038/ng0498-345>
- Raghu P, Joseph A, Krishnan H et al (2019) Phosphoinositides: regulators of nervous system function in health and disease. *Front Mol Neurosci* 12:208. <https://doi.org/10.3389/fnmol.2019.00208>
- Ramos AR, Ghosh S, Suhel T et al (2019) Phosphoinositide 5-phosphatases SKIP and SHIP2 in ruffles, the endoplasmic reticulum and the nucleus: an update. *Adv Biological Regul* 75:100660. <https://doi.org/10.1016/j.jbior.2019.100660>
- Ravi V, Venkatesh B (2018) The divergent genomes of teleosts. *Annu Rev Anim Biosci* 6:47–68. <https://doi.org/10.1146/annurev-animal-030117-014821>
- Sémon M, Wolfe KH (2007) Consequences of genome duplication. *Curr Opin Genet Dev* 17:505–512. <https://doi.org/10.1016/j.gde.2007.09.007>
- Senderek J, Krieger M, Stendel C et al (2005) Mutations in SIL1 cause Marinesco-Sjögren syndrome, a cerebellar ataxia with cataract and myopathy. *Nat Genet* 37:1312–1314. <https://doi.org/10.1038/ng1678>
- Sievers F, Wilm A, Dineen D et al (2011) Fast, scalable generation of high-quality protein multiple sequence alignments using Clustal Omega. *Mol Syst Biol* 7:539–539. <https://doi.org/10.1038/msb.2011.75>
- Tréaues L, Silvester C, Flodin S et al (2014) Structural basis for phosphoinositide substrate recognition, catalysis, and membrane interactions in human inositol polyphosphate 5-phosphatases. *Structure* 22:744–755. <https://doi.org/10.1016/j.str.2014.01.013>
- Vandeput F, Backers K, Villeret V et al (2006) The influence of anionic lipids on SHIP2 phosphatidylinositol 3,4,5-trisphosphate 5-phosphatase activity. *Cell Signal* 18:2193–2199. <https://doi.org/10.1016/j.cellsig.2006.05.010>

- Vatine G, Vallone D, Gothilf Y, Foulkes NS (2011) It's time to swim! Zebrafish and the circadian clock. *Febs Lett* 585:1485–1494. <https://doi.org/10.1016/j.febslet.2011.04.007>
- Waterhouse AM, Procter JB, Martin DMA et al (2009) Jalview Version 2—a multiple sequence alignment editor and analysis workbench. *Bioinformatics* 25:1189–1191. <https://doi.org/10.1093/bioinformatics/btp033>
- Wiessner M, Roos A, Munn CJ et al (2017) Mutations in INPP5K, encoding a phosphoinositide 5-phosphatase, cause congenital muscular dystrophy with cataracts and mild cognitive impairment. *Am J Hum Genet* 100:523–536. <https://doi.org/10.1016/j.ajhg.2017.01.024>
- Yamagata M, Yan W, Sanes JR (2021) A cell atlas of the chick retina based on single-cell transcriptomics. *Elife* 10:e63907. <https://doi.org/10.7554/elif.63907>
- Yan B, Neilson KM, Moody SA (2009) foxD5 plays a critical upstream role in regulating neural ectodermal fate and the onset of neural differentiation. *Dev Biol* 329:80–95. <https://doi.org/10.1016/j.ydbio.2009.02.019>
- Yousaf S, Sheikh SA, Riazuddin S, et al (2017) INPP5K variant causes autosomal recessive congenital cataract in a Pakistani family. *Clinical Genetics*. <https://doi.org/10.1111/cge.13143>
- Zhao X-F, Ellingsen S, Fjose A (2009) Labelling and targeted ablation of specific bipolar cell types in the zebrafish retina. *Bmc Neurosci* 10:107. <https://doi.org/10.1186/1471-2202-10-107>

Publisher's note Springer Nature remains neutral with regard to jurisdictional claims in published maps and institutional affiliations.